This article has been accepted for publication in a future issue of this journal, but has not been fully edited. Content may change prior to final publication. Citation information: DOI 10.1109/TBME.2019.2932808, IEEE Transactions on Biomedical Engineering

Theoretical Value of Deceleration Capacity Points to Deceleration Reserve of Fetal Heart Rate

Massimo W. Rivolta, *Member, IEEE,* Tamara Stampalija, Martin G. Frasch, and Roberto Sassi, *Senior Member, IEEE*

***Abstract*—Objective: The interpretation of Average Acceleration and Deceleration Capacities (AC/DC), computed through Phase-Rectified Signal Averaging (PRSA), in intrapartum fetal heart rate (FHR) monitoring is still matter of investigation. We aimed to elucidate some behaviours of AC/DC. Methods: We derived the theoretical value of PRSA for stationary stochastic Gaussian processes and proved that for these time series AC and DC are necessarily identical in absolute value. The difference between DC and AC, termed Deceleration Reserve (DR), was introduced to detect signals asymmetric trends. DR was tested on FHR signals from: near-term pregnant sheep model of labor consisting of chronically hypoxic and normoxic fetuses with both groups developing acidemia due to umbilical cord occlusions (UCO); and the CTU-UHB dataset containing fetal CTG recordings collected during labor of newborns that resulted acidotic and non-acidotic, respectively. DR was compared with AC and DC in terms of discriminatory power (AUC), between the groups, after correcting for signals power or deceleration area, respectively. Results: DR displayed higher discriminatory power on the animal model during severe acidemia, with respect to AC/DC ($p < 0.05$) but also distinguished correctly all chronically hypoxic from normoxic fetuses at baseline prior to UCO. DR also outperformed AC/DC on the CTU-UHB dataset in distinguishing acidemic fetuses at birth (AUC: 0.65). Conclusion: Theoretical results motivated the introduction of DR, that proved to be superior than AC/DC for risk stratification during labor. Significance: DR, measured during labor, might permit to distinguish acidemic fetuses due to their different autonomic regulation, paving the way for new monitoring strategies.**

***Index Terms*—phase-rectified signal averaging (PRSA), fetal heart rate variability, fetal monitoring, heart rate variability**

I. Introduction

AVERAGE Acceleration and Deceleration Capacity (AC, DC) of heart rate [1] are quantified on inter-beat interval series (RR) through the Phase-Rectified Signal Averaging (PRSA) technique, proposed by Bauer *et al.* [2]. The two indexes gained significant acceptance in the biomedical engineering community for their robustness to signal quality (noise) and for their proven sensitivity to diverse clinical conditions, such as myocardial infarction, fetal distress, heart failure, dilated cardiomyopathy *etc.* [1], [3], [4], [5], [6], [7].

Given the fact that they measure the "capacity" of the heart rate to increase or decrease, it might be tempting to associate AC and DC to the sympathetic and vagal autonomic activity, respectively. However, many studies have reported identical values of AC and DC in the same experimental conditions [8], [3], [5]. In addition, recent studies based on mathematical models [9], [10] further corroborated the hypothesis that AC and DC might measure the same aspects of the autonomic regulation. For example, the realistic cardiovascular system model of Ursino and Magosso [11], including several major aspects of the cardiovascular system, such as systemic and pulmonary circulations, sympathetic feedback control loops and sympatho-vagal control of heart period, was investigated by Pan *et al.* [10] to assess the role of short-term regulations on AC and DC values. In this condition, DC and AC provided similar information in terms of autonomic control.

Clinical evidences and findings on mathematical models make thus unclear to what extent AC and DC might be directly linked to autonomic modulators on short time spans. On the other hand, on long time scales, it is likely that the physiological mechanisms responsible for acceleration and deceleration of heart rate might be different, at least on longer time scales, as patients with degraded DC and preserved AC were found to have poor outlook, *e.g.*, after myocardial infarction in a large clinical study [1].

A technical aspect that complicates the physiological understanding of AC and DC is their dependence on three parameters (T, s and, to a minor extent L, which needs to be greater or equal than both T and s, see section II-A). In particular, T and s allow to capture different oscillations, with T selecting their locations in time, and s their periodicities. For example, for some combinations of these parameters values (*e.g.*, $T = 1$, $s = 2$), both DC and AC appeared solely dependent on vagal activity, whereas with others (*e.g.*, $T = 3$, $s = 5$), both DC and AC were also linked to sympathetic activity [10].

To partly address the issue, in a preliminary work [9], we employed synthetic RR series, each with a specific spectral content, to show that the value of s, more than T, selects the frequency band (centered at $f \approx 0.371 f_s/s$, where f_s is the sampling rate) which lead to larger AC or DC values. We also speculated, based on the results of the simulations, that a difference between the values of AC and DC cannot depend on the shape of the power spectrum. In fact, for the series $x[n]$ and its time-reversed version $x[-n]$, the magnitudes of the discrete-time Fourier transform are identical but, on the other hand, accelerations turn into decelerations (and AC into DC) when time is reversed. Thus, AC and DC are identical both when the power spectrum of a stationary series displays a large low-frequency component (typically linked to the activation of

M. W. Rivolta and R. Sassi are with the Dipartimento di Informatica, Università degli Studi di Milano, 20133, Milano, Italy. Corresponding author's email: massimo.rivolta@unimi.it.

T. Stampalija is with the Unit of Fetal Medicine and Prenatal Diagnosis, Institute for maternal and child health IRCCS Burlo Garofolo, Trieste, Italy.

M. Frasch is with the Department of Obstetrics and Gynecology, University of Washington, Seattle (WA), USA.

0018-9294 (c) 2019 IEEE. Personal use is permitted, but republication/redistribution requires IEEE permission. See http://www.ieee.org/publications_standards/publications/rights/index.html for more information.

This article has been accepted for publication in a future issue of this journal, but has not been fully edited. Content may change prior to final publication. Citation information: DOI 10.1109/TBME.2019.2932808, IEEE Transactions on Biomedical Engineering

the sympathetic branch of the ANS), and when high-frequency oscillations (associated to the vagal activity) dominate.

To move a significant step forward in clarifying the physiological understanding of AC and DC, in the first part of this paper, we showed that it is possible to derive an analytical closed-form expression of the values of AC and DC for stationary stochastic Gaussian processes. The theoretical formulation proves that AC and DC are indeed identical for such processes. The result is, in our opinion, of seminal importance. For example, it justifies why they might assume similar values, when the RR series appear stationary.

On the other hand, the difference between AC and DC might uncover departures from stationarity and Gaussianity, with a possible diagnostic value. Thus, we introduced a new PRSA-based index sensitive to the unbalancing between deceleration and acceleration capacities, which we termed Deceleration Reserve (DR). Apart from the theoretical results reported in the first part of the manuscript, DR was also inspired by the works on the effects of heart rate asymmetry on AC and DC performed by Karmakar *et al.* [12] and Pan *et al.* [13]. In particular, the former study focused on fetal heart rate (FHR) and this is the domain in which we will also test our findings and new index.

FHR represents the current standard for the evaluation of the fetus' well-being in pregnancy monitoring. Despite the progress obtained with computerized FHR monitoring in preventing life-threatening events, it is still difficult to promptly predict fetal hypoxia or acidosis. Even when exploiting the information coming from multiple indexes [14], [15], or when using recent deep learning strategies [16], [17], the prediction accuracy displays a high variability across studies (accuracies might vary from 60% to 90%, but in the latter case sensitivity can be as low as 56%). AC and DC achieved promising results in FHR monitoring, being capable to differentiate healthy fetuses and those with growth restriction [8], [18], [5], even at different gestational age epochs [3]. Additionally, significative correlations between AC and DC and biomarkers of hypoxia were found in a near-term animal model of labor [19]. Therefore, in the second part of this study, we tested the suitability of DR in detecting hypoxia from FHR series, where heart rate asymmetry might play a significant role.

DR was tested on two different datasets. The first one comprises two *in*-vivo near-term pregnant sheep models (one normoxic and one chronically hypoxic) [20]. It was used to assess the correlation between DR and three biomarkers, *i.e.*, pH, lactate, base deficit, and to determine the DR's discriminatory power by means of ROC analysis. The second one is a dataset collected intrapartum and used to rank DR, AC and DC based on their discriminatory power in detecting fetal acidemia at birth [21].

II. Methods

A. Definition of AC and DC

Acceleration and Deceleration Capacities are computed through the Phase-Rectified Signal Averaging (PRSA) technique introduced by Bauer *et al.* [2], [22]. PRSA is meant to provide an estimate of the autonomic regulation of the HR even when phase de-synchronizations, due to abrupt changes in the system, miss-detected beats and signal losses, are present.

In order to compute DC on the RR series, all the time points t such that

$$A_{\mathrm{DC}} = \left\{ t : \frac{1}{T}\sum_{i=0}^{T-1} \mathrm{RR}[t+i] > \frac{1}{T}\sum_{i=1}^{T} \mathrm{RR}[t-i] \right\} \quad (1)$$

are termed "anchor points". The integer value T sets the "timescale" and the set A_{DC} is the "decelerations' list". The "accelerations' list" A_{AC} is instead built by changing the direction of the inequality in (1).

A window of length $2L$ samples is centered on each anchor point (the anchor point is at position $L+1$). Then, the windows (one for each anchor point) are aligned and averaged, obtaining the PRSA series. Finally, the PRSA series is used to compute the DC with

$$\mathrm{DC} = \frac{1}{2s}\sum_{i=1}^{s} \mathrm{PRSA}[L+i] - \frac{1}{2s}\sum_{i=0}^{s-1} \mathrm{PRSA}[L-i] \quad (2)$$

where s is the scale. AC is computed with the same formula, but with a different PRSA series obtained using the accelerations' list A_{AC}.

Summarizing, the three parameters T, L and s need to be specified when computing AC or DC. T sets the number of points of the low-pass moving average filter used to detect the anchor points. L determines the span of the PRSA series and it needs to be larger than the period of the slowest oscillation to be detected with PRSA. The scale s selects the oscillations in the PRSA series that most affect AC and DC. Further details on their effect can be found in [9].

B. Theoretical Value of AC and DC for Gaussian stationary processes

Given a realization of a stochastic process, the procedure outlined in the previous section can be applied to compute its associated PRSA series. Clearly, the estimated PRSA series might slightly change while selecting a different realization of the same process. However, the expected value of the PRSA series is strictly linked to the properties of the stochastic process itself. In this section, we derive the value of the theoretical (expected) value of the PRSA series associated to a given stationary Gaussian stochastic process X, with mean $\mu_X = 0$ and autocorrelation function $\rho_X(k)$. Without lack of generality we deal with decelerations first and give an equivalent formula for accelerations at the end of section.

Exploiting the fact that a stationary Gaussian process is also ergodic, in place of using time-averages to estimate PRSA values, we use ensemble averages instead. Therefore, let us consider $2L$ consecutive samples, $\mathbf{x} = [x_1, x_2, \ldots, x_{2L}]^\intercal$ (where $^\intercal$ is the transpose operator). The joint probability density function of $\mathbf{x}$ is

$$\mathrm{pdf}_X(\mathbf{x}) = \frac{(\det \boldsymbol{\Sigma}_{\mathbf{x}})^{-\frac{1}{2}}}{(2\pi)^L} e^{-\frac{1}{2}\mathbf{x}^\intercal \boldsymbol{\Sigma}_{\mathbf{x}}^{-1}\mathbf{x}}$$

where $\boldsymbol{\Sigma}_{\mathbf{x}}$ is a covariance matrix built using the first $2L$ values of $\rho_X(k)$.

0018-9294 (c) 2019 IEEE. Personal use is permitted, but republication/redistribution requires IEEE permission. See http://www.ieee.org/publications_standards/publications/rights/index.html for more information.

This article has been accepted for publication in a future issue of this journal, but has not been fully edited. Content may change prior to final publication. Citation information: DOI 10.1109/TBME.2019.2932808, IEEE Transactions on Biomedical Engineering

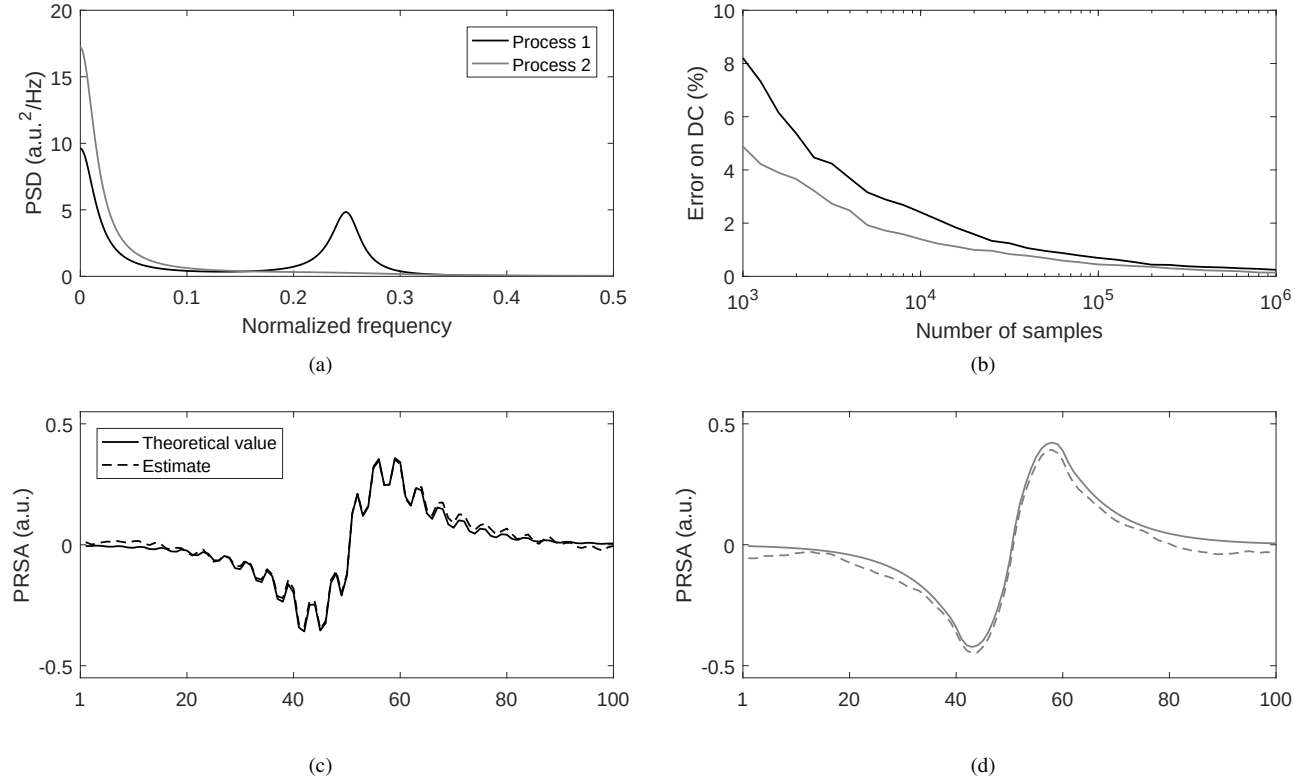

Fig. 1. Panel a) Power spectral density of the two autoregressive processes used in the simulations. Panel b) average percentage error on DC (difference between the DC theoretical and estimated values, over 100 random repetitions). Panel c) theoretical value of the PRSA series and its estimate (dashed line), obtained from a series of 7500 samples for the first process. Panel d) as panel c) but for the second process. a.u. refers to the unit of the input signal. Bold lines refer to process 1, with prominent high frequency components. Simulations were performed with $T = 10$, $L = 50$ and $s = 1$.

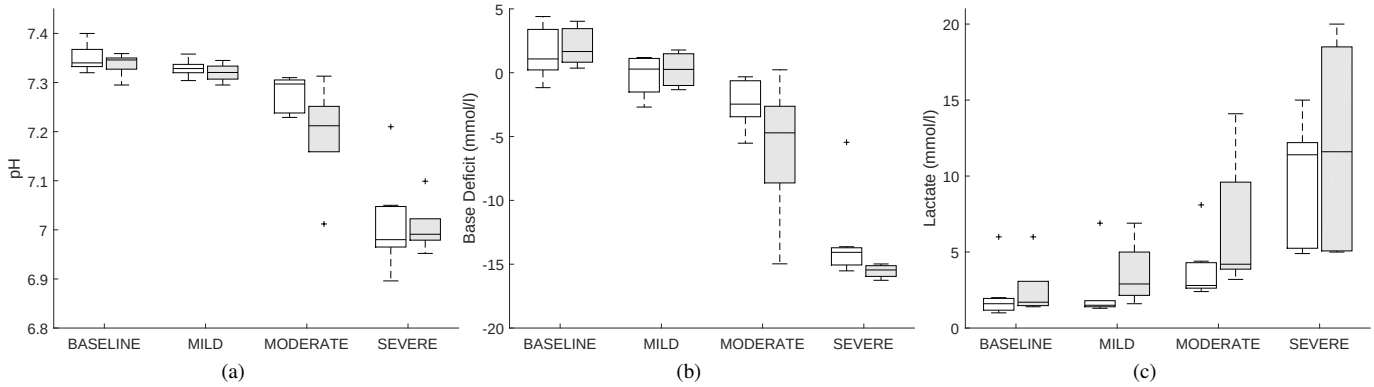

Fig. 2. Boxplot of the three biomarkers for each protocol phase in both normoxic (white) and chronically hypoxic (light grey) sheep. BASELINE refers to measures collected before the onset of the UCO stimulation protocol.

Using ensemble averages instead of time averages, anchor points in (1) are mapped to the region $\mathcal{A}_{\mathrm{DC}}$ in the $2L$-dimensional space where $\sum_{i=1}^{T} x_{L+i} > \sum_{i=0}^{T-1} x_{L-i}$ (the anchor point, AP, is conventionally located in position x_{L+1}). Equivalently:

$$\mathcal{A}_{\mathrm{DC}} = \{\mathbf{x} : \mathbf{g}^{\intercal}\mathbf{x} > 0\}$$
$$\mathbf{g} = [0, \cdots, 0, \underbrace{-1, \cdots, -1}_{T \text{ values}}, \overbrace{\underbrace{1}_{\text{AP}}, \cdots, 1}^{T \text{ values}}, 0, \cdots, 0]^{\intercal}. \quad (3)$$

The PRSA series can be determined as the expected value of $\mathbf{x}$ over one of the two hyperspaces defined by $\mathbf{g}$. It can be computed, for each sample i, as follows

$$\mathrm{PRSA}[i] = \mathrm{E}[x_i]|_{\mathbf{x}\in\mathcal{A}_{\mathrm{DC}}} = 2 \int_{\mathbf{g}^{\intercal}\mathbf{x}>0} \mathbf{e}_i^{\intercal}\mathbf{x}\,\mathrm{pdf}_X(\mathbf{x})d\mathbf{x}, \quad (4)$$

where $\mathbf{e}_i$ is the i^{th} unitary vector (which is one only at position i and zero otherwise). The factor 2 is necessary to normalize the pdf (only half of the space is considered). In order to compute analytically the integral in (4), two changes of variables are instrumental. First, considering that $\mathbf{\Sigma_x}$ is a positive semi-definite matrix, we can factorize it by using a product of an

0018-9294 (c) 2019 IEEE. Personal use is permitted, but republication/redistribution requires IEEE permission. See http://www.ieee.org/publications_standards/publications/rights/index.html for more information.

This article has been accepted for publication in a future issue of this journal, but has not been fully edited. Content may change prior to final publication. Citation information: DOI 10.1109/TBME.2019.2932808, IEEE Transactions on Biomedical Engineering

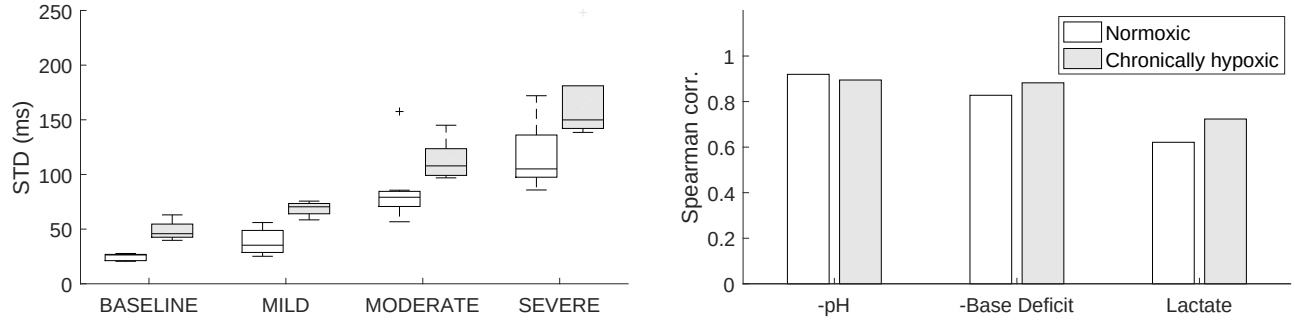

(a) (b)

Fig. 3. Panel (a): FRR standard deviation (STD) across protocol phases. The larger standard deviation in the chronically hypoxic model is due to a greater reduction of FHR during UCOs. Panel (b): Absolute value of the Spearman correlation between STD and biomarkers, for both normoxic (left) and chronically hypoxic (right) sheep.

orthogonal and diagonal matrix, *i.e.*, $\mathbf{\Sigma_x} = \mathbf{UDU}^\intercal$, where $\mathbf{U}$ is a matrix containing the eigenvectors of $\mathbf{\Sigma_x}$ and $\mathbf{D}$ is the diagonal matrix of eigenvalues. Then, performing the variable change $\mathbf{y} = \mathbf{D}^{-\frac{1}{2}}\mathbf{U}^\intercal\mathbf{x}$, (4) becomes:

$$\mathrm{PRSA}[i] = \frac{2}{(2\pi)^L} \int\limits_{\mathbf{w}^\intercal\mathbf{y}>0} \boldsymbol{\varepsilon}_i^\intercal \mathbf{y} e^{-\frac{1}{2}\mathbf{y}^\intercal\mathbf{y}} d\mathbf{y} \tag{5}$$

where $\mathbf{w} = \mathbf{D}^{\frac{1}{2}}\mathbf{U}^\intercal\mathbf{g}$, $\boldsymbol{\varepsilon}_i = \mathbf{D}^{\frac{1}{2}}\mathbf{U}^\intercal\mathbf{e}_i$ and $\det\mathbf{U} = 1$ as it is a special orthogonal matrix. This procedure is equivalent to the whitening of the statistical process X (similar to that commonly performed when using Principal Component Analysis). Indeed, the covariance matrix of the stochastic process Y, obtained with the linear transformation, is the identity matrix.

With the second change of variables $\mathbf{z} = \mathbf{Hy}$, the probability density function of Y is rotated such that the hyperplane defined by $\mathbf{w}$, separating the two regions containing either anchor points or not, becomes orthogonal to one of the canonical axes (without lack of generality, we select the $L+1$ one, *i.e.*, $\mathbf{e}_{L+1}$, so that it is at the conventional location of the anchor point). This operation can be achieved with the Householder transformation, that is an orthogonal matrix $\mathbf{H}$ such that

$$\mathbf{Hw} = \|\mathbf{w}\|\mathbf{e}_{L+1},$$

where $\mathbf{H}$ is given by[1]

$$\begin{aligned} \mathbf{v} &= \mathbf{w} - \|\mathbf{w}\|\mathbf{e}_{L+1} \\ \mathbf{H} &= \mathbf{I} - 2\frac{\mathbf{vv}^\intercal}{\mathbf{v}^\intercal\mathbf{v}} \end{aligned} \tag{6}$$

and $\mathbf{I}$ is the identity matrix. The integral in (5) becomes

$$\begin{aligned} \mathrm{PRSA}[i] &= \frac{2}{(2\pi)^L} \int\limits_{\|\mathbf{w}\|\mathbf{e}_{L+1}^\intercal\mathbf{z}>0} \boldsymbol{\varepsilon}_i^\intercal\mathbf{H}^\intercal\mathbf{z} e^{-\frac{1}{2}\mathbf{z}^\intercal\mathbf{z}} |\det\mathbf{H}| d\mathbf{z} \\ &= \frac{2}{(2\pi)^L} \int\limits_{z_{L+1}>0} \boldsymbol{\varepsilon}_i^\intercal\mathbf{H}^\intercal\mathbf{z} e^{-\frac{1}{2}\mathbf{z}^\intercal\mathbf{z}} d\mathbf{z} \\ &= \sqrt{\frac{2}{\pi}}\mathbf{e}_{L+1}^\intercal\mathbf{H}\boldsymbol{\varepsilon}_i = \sqrt{\frac{2}{\pi}}\mathbf{e}_{L+1}^\intercal\mathbf{H}\mathbf{D}^{\frac{1}{2}}\mathbf{U}^\intercal\mathbf{e}_i, \end{aligned} \tag{7}$$

[1]When the vector $\mathbf{v}$, provided by (6), is a zero vector $\mathbf{0}$, it is necessary to use an alternative formulation of the Householder transformation, with $\mathbf{v} = \mathbf{w} + \|\mathbf{w}\|\mathbf{e}_{L+1}$ and $\mathbf{H} = -\mathbf{I} + 2\mathbf{vv}^\intercal/(\mathbf{v}^\intercal\mathbf{v})$.

given that $|\det\mathbf{H}| = 1$ as $\mathbf{H}$ is an orthogonal matrix. In vector form, (7) can be rewritten as

$$\begin{aligned} \mathrm{PRSA} &= \left(\sqrt{\frac{2}{\pi}}\mathbf{e}_{L+1}^\intercal\mathbf{H}\mathbf{D}^{\frac{1}{2}}\mathbf{U}^\intercal\mathbf{I}\right)^\intercal \\ &= \sqrt{\frac{2}{\pi}}\mathbf{U}\mathbf{D}^{\frac{1}{2}}\mathbf{H}^\intercal\mathbf{e}_{L+1} = \mathbf{p}. \end{aligned} \tag{8}$$

A wavelet transform (using a Haar mother wavelet function) of the PRSA series, evaluated at scale s (the third free parameter) and location $L+1$, is employed to derive the capacities as in (2). Given

$$\mathbf{h} = [0, \cdots, 0, \underbrace{-1, \cdots, -1}_{s \text{ values}}, \underbrace{1, \cdots, 1}_{s \text{ values}}, 0, \cdots, 0]^\intercal.$$

then

$$\mathrm{DC} = \frac{1}{2s}\mathbf{h}^\intercal\mathbf{p}. \tag{9}$$

The quantity in (9) is the theoretical value of deceleration capacity for a series generated by a Gaussian stationary stochastic process. For acceleration capacity, the procedure which has to be followed is identical, with the exception of (3), where $\mathcal{A}_{\mathrm{DC}}$ is replaced by

$$\mathcal{A}_{\mathrm{AC}} = \{\mathbf{x} : -\mathbf{g}^\intercal\mathbf{x} > 0\}.$$

The change of sign in $\mathbf{g}$ leads into the following equations, and given the fact that the $2L$-dimensional space is partitioned into two identical parts, then

$$\mathrm{AC} = -\frac{1}{2s}\mathbf{h}^\intercal\mathbf{p}. \tag{10}$$

Comparing (10) and (9), it is clear that for a stationary stochastic Gaussian process AC and DC are identical in magnitude and $\mathrm{AC} = -\mathrm{DC}$.

As a final remark, the theoretical framework outlined in this section can be used to clarify other characteristics of AC and DC. A couple are verified in the appendix. In particular, while the average number of anchor points found in a given series might depend on T, for realizations of a stationary stochastic Gaussian process, half of the samples are anchor points for AC and the other half are anchor points for DC (see App. A). Also, it is possible to prove what was speculated in [9], that is, for a stationary stochastic Gaussian process, after time-reversal AC turns into -DC (and viceversa, see App. B).

0018-9294 (c) 2019 IEEE. Personal use is permitted, but republication/redistribution requires IEEE permission. See http://www.ieee.org/publications_standards/publications/rights/index.html for more information.

This article has been accepted for publication in a future issue of this journal, but has not been fully edited. Content may change prior to final publication. Citation information: DOI 10.1109/TBME.2019.2932808, IEEE Transactions on Biomedical Engineering

TABLE I
AC, DC AND DR VALUES (MEDIAN AND INTERQUARTILE RANGE) FOR NORMOXIC AND CHRONICALLY HYPOXIC SHEEP IN EACH PROTOCOL PHASE (NOT CORRECTED FOR SIGNAL'S POWER).

a) Normoxic	T	s	BASELINE	MILD	MODERATE	SEVERE
AC	1	2	-2.0 (-2.3, -1.7)	-2.2 (-2.6, -1.8)	-3.7 (-5.2, -2.9)	-7.2 (-8.9, -5.2)
DC	1	2	2.2 (2.0, 2.8)	2.5 (2.0, 3.1)	4.6 (3.5, 5.9)	8.3 (5.5, 11.6)
AC	5	5	-3.3 (-3.8, -2.7)	-3.7 (-3.9, -3.5)	-6.2 (-7.7, -5.7)	-12.0 (-15.0, -9.0)
DC	5	5	3.4 (2.9, 4.4)	4.0 (3.6, 4.5)	7.6 (6.1, 9.2)	12.1 (9.7, 14.7)
AC	9	9	-4.0 (-4.1, -3.3)	-4.5 (-4.7, -4.0)	-7.9 (-8.8, -7.8)	-12.1 (-16.6, -11.2)
DC	9	9	3.9 (3.4, 4.9)	4.6 (4.5, 5.7)	9.8 (9.1, 11.5)	15.0 (13.3, 17.4)
AC	40	1	-0.4 (-0.4, -0.3)	-0.4 (-0.5, -0.3)	-0.6 (-0.7, -0.5)	-1.0 (-1.1, -0.7)
DC	40	1	0.4 (0.3, 0.4)	0.5 (0.4, 0.5)	1.0 (0.9, 1.4)	2.1 (1.5, 3.8)
DR	1	2	0.3 (0.2, 0.3)	0.3 (0.2, 0.4)	0.7 (0.4, 0.8)	1.1 (0.6, 2.1)
DR	5	5	0.1 (0.0, 0.6)	0.3 (0.1, 0.5)	1.0 (0.6, 1.4)	0.7 (0.2, 1.8)
DR	5	1	0.0 (0.0, 0.2)	0.2 (0.0, 0.3)	0.4 (0.3, 0.5)	0.6 (0.2, 1.4)
DR	9	9	0.0 (-0.2, 0.4)	0.3 (0.1, 0.6)	1.7 (1.3, 2.7)	2.1 (1.5, 4.7)
DR	9	1	0.0 (-0.0, 0.1)	0.1 (0.0, 0.2)	0.5 (0.4, 0.6)	0.8 (0.4, 1.8)
DR	40	1	0.0 (-0.0, 0.0)	0.1 (0.0, 0.1)	0.5 (0.4, 0.8)	1.1 (0.3, 2.9)
b) Chronically hypoxic						
AC	1	2	-2.8 (-3.2, -2.4)	-3.1 (-3.5, -2.5)	-5.9 (-8.1, -4.3)	-8.0 (-12.5, -8.0)
DC	1	2	3.5 (3.0, 3.9)	3.9 (3.2, 4.4)	7.1 (5.8, 8.4)	9.7 (8.1, 12.1)
AC	5	5	-4.9 (-5.3, -4.1)	-5.5 (-6.5, -4.3)	-10.0 (-12.2, -6.9)	-13.4 (-18.2, -13.0)
DC	5	5	5.3 (4.5, 5.9)	6.2 (5.1, 7.6)	9.8 (8.8, 12.3)	12.4 (10.7, 16.4)
AC	9	9	-5.6 (-6.1, -4.7)	-6.5 (-7.5, -5.5)	-11.7 (-14.8, -8.9)	-16.3 (-20.3, -15.6)
DC	9	9	5.6 (5.0, 6.4)	7.2 (6.3, 9.1)	12.3 (10.9, 15.1)	14.7 (13.8, 21.1)
AC	40	1	-1.3 (-1.9, -1.1)	-1.2 (-1.4, -0.9)	-1.5 (-1.8, -1.4)	-1.9 (-4.8, -1.6)
DC	40	1	1.3 (1.1, 1.9)	1.3 (1.1, 1.8)	2.0 (1.6, 2.7)	1.5 (1.3, 3.8)
DR	1	2	0.6 (0.5, 0.8)	0.8 (0.5, 1.1)	1.0 (0.3, 1.3)	-0.2 (-0.7, 0.7)
DR	5	5	0.6 (0.4, 0.6)	0.8 (0.4, 1.5)	1.3 (-0.5, 1.6)	-1.3 (-2.2, -1.2)
DR	5	1	0.3 (0.2, 0.4)	0.4 (0.2, 0.8)	0.7 (-0.2, 1.2)	-1.0 (-1.7, -1.0)
DR	9	9	0.4 (0.1, 0.6)	0.8 (0.5, 2.0)	1.6 (-0.4, 2.7)	-0.1 (-1.8, 1.0)
DR	9	1	0.1 (0.0, 0.2)	0.3 (0.2, 0.7)	0.6 (-0.1, 1.0)	-0.7 (-1.5, -0.1)
DR	40	1	0.0 (-0.0, 0.1)	0.2 (0.1, 0.5)	0.2 (0.0, 1.0)	-0.4 (-0.9, 0.5)

C. A relevant case: $T = 1$ and $s = 1$

A relevant applicative case is when $T = 1$ and also $s = 1$; it then also suffices to consider $L = \max(s, T) = 1$. Let the $2L = 2$ dimensional covariance matrix of the stationary sthocastic Gaussian process be

$$\mathbf{\Sigma_x} = \sigma^2 \begin{bmatrix} 1 & \rho \\ \rho & 1 \end{bmatrix},$$

where ρ is the lag 1 correlation coefficient between x_k and x_{k+1}, and σ^2 is the variance. The eigenvalues of $\mathbf{\Sigma_x}$ are $\sigma^2(1+\rho)$ and $\sigma^2(1-\rho)$, while the corresponding eigenvectors are $[1/\sqrt{2}, 1/\sqrt{2}]^\intercal$ and $[1/\sqrt{2}, -1/\sqrt{2}]^\intercal$. With respect to decelerations, it is then straightforward that $\mathbf{g} = [-1, 1]^\intercal$, $\mathbf{w} = [0, -\sigma\sqrt{2(1-\rho)}]^\intercal$, $\mathbf{v} = 2\mathbf{w}$, and $\mathbf{H}$ is a diagonal matrix with $H_{11} = 1$ and $H_{22} = -1$. Given that $\mathbf{H}\mathbf{e}_{L+1} = -\mathbf{e}_2$ and $\mathbf{h} = [-1, 1]^\intercal$,

$$\mathrm{DC} = \sigma\sqrt{\frac{1-\rho}{\pi}}.$$

Considering accelerations, $\mathbf{w} = [0, \sigma\sqrt{2(1-\rho)}]^\intercal$ and $\mathbf{v} = 2\mathbf{w}$ (using the alternative formulation of the Householder transformation), while $\mathbf{H}$ is a diagonal matrix with $H_{11} = -1$ and $H_{22} = 1$. Therefore, $\mathbf{H}\mathbf{e}_{L+1} = \mathbf{e}_2$ and

$$\mathrm{AC} = -\sigma\sqrt{\frac{1-\rho}{\pi}}.$$

As expected, AC and DC only differ in sign. Both linearly depend on the standard deviation of the series and reach the maximum when the process is strongly anti-correlated. For a white Gaussian noise, $\rho = 0$ and $-\mathrm{AC} = \mathrm{DC} = \sigma/\sqrt{\pi}$.

D. Comparison with numerical simulations

For illustration, and as a further check, we compared the PRSA series predicted for a stationary stochastic Gaussian process by (8) and its estimate obtained using the algorithm described in section II-A, on a synthetic series generated by the same process. Specifically, we considered two autoregressive processes having different power spectral densities (reported in Fig. 1a). The transfer functions of the processes were $1/(1 - 0.9z^{-1} + 0.81z^{-2} - 0.729z^{-3})$ and $1/(1 - 0.9z^{-1} + 0.25z^{-2} - 0.225z^{-3})$, while the variance of the input noise was set so that the power $\sigma^2 = 1$. Empirically, we set $L = 50$, $T = 10$ and $s = 1$.

Fig. 1c and 1d contain the predicted values of PRSA and a numerical estimate obtained from a single series of 7500 samples (dashed lines), for both processes: the matching is evident. Moreover, when increasing the number of samples, the estimated PRSA series converged to its theoretical value (in terms of mean square error). This is confirmed by the decreasing average percentage error on DC reported in Fig. 1b, which displays an average computed over 100 Monte Carlo runs.

Interestingly, Fig. 1c strongly resembles the Fig. 2c contained in the original paper of Bauer *et al.* [2]. As clearly visible, the relevant frequency components of the original RR series are enhanced in the PRSA series.

0018-9294 (c) 2019 IEEE. Personal use is permitted, but republication/redistribution requires IEEE permission. See http://www.ieee.org/publications_standards/publications/rights/index.html for more information.

This article has been accepted for publication in a future issue of this journal, but has not been fully edited. Content may change prior to final publication. Citation information: DOI 10.1109/TBME.2019.2932808, IEEE Transactions on Biomedical Engineering

TABLE II
SPEARMAN'S CORRELATION COEFFICIENT BETWEEN POWER-CORRECTED AC, DC, DR VALUES AND BIOMARKERS CONSIDERING THE ENTIRE EXPERIMENT, IN THE TWO FETAL SHEEP MODELS (* REFERS TO $p < 0.05$). CHR. STANDS FOR "CHRONICALLY".

			pH		Lactate		Base Deficit	
	T	s	NORMOXIC	CHR. HYPOXIC	NORMOXIC	CHR. HYPOXIC	NORMOXIC	CHR. HYPOXIC
AC	1	2	0.0	0.6*	0.0	−0.6*	−0.1	0.6*
DC	1	2	−0.1	−0.3	0.0	0.5	0.0	−0.2
AC	5	5	0.0	0.6*	0.0	−0.6*	−0.1	0.6*
DC	5	5	−0.2	0.0	0.0	0.3	0.0	0.1
AC	9	9	0.1	0.5*	−0.1	−0.5*	0.0	0.5*
DC	9	9	−0.3	0.0	0.1	0.3	−0.1	0.1
AC	40	1	−0.5*	−0.1	0.3	−0.1	−0.5*	−0.2
DC	40	1	0.0	0.4	0.0	−0.1	0.1	0.6*
DR	1	2	−0.5*	0.5*	0.1	−0.5	−0.3	0.5*
DR	5	5	−0.4	0.6*	0.0	−0.4	−0.2	0.7*
DR	5	1	−0.5*	0.6*	0.3	−0.4	−0.3	0.6*
DR	9	9	−0.4*	0.5	0.1	−0.2	−0.3	0.6*
DR	9	1	−0.5*	0.6*	0.3	−0.3	−0.3	0.6*
DR	40	1	−0.5*	0.4	0.4	0.0	−0.4*	0.4

E. Deceleration Reserve

The results of the previous sections highlighted that when the time series can be reasonably generated by a stationary stochastic Gaussian process, AC and DC are identical in absolute value and, therefore, cannot provide different information on the series. However, since the work of Bauer *et al.* [1], it has been clear that differences in AC and DC bear a relevant discriminative power. Dissimilarities in AC and DC values arise when asymmetric increasing or decreasing trends appear in the signal [9], a situation which is common in FHR during labor. Also, capacities might differ from each other in presence of non-stationarities and non-gaussianities.

Motivated by these considerations, we believed it was relevant to introduce a new PRSA-based index, which we termed *Deceleration Reserve* (DR), given by the difference between DC and AC:

$$\mathrm{DR} = \mathrm{DC} + \mathrm{AC}$$

(please recall that AC is a negative quantity on RR series). Obviously, DR, as well as AC and DC, also depends on the parameters L, T and s. DR reflects whether the average growth in the time series is mainly constituted by growing (DR is positive) or decaying trends (DR is negative).

III. EXPERIMENTS AND RESULTS

In this section, we tested the DR index on two datasets containing fetal RR series (FRR) collected during labor. The main rationale was that fetal stress during delivery is known to produce changes in the fetal heart rate due to the presence of contractions of the woman's womb. These periodic contractions produce repeated decelerations and subsequent recoveries of the fetal heart rate. Moreover, one of the major harmful conditions for the fetus is the lack of oxygen (hypoxemia and hypoxia) and metabolites that might persist over time during the entire course of the labor resulting in acidemia. This severe condition is usually associated with the presence of specific patterns of FRR.

Here, the main goal was twofold. First, we determined whether the DR index was correlated with common measurements of fetal distress using an animal model. Second, we compared the DR index with AC and DC in terms of discrimination power between healthy and acidotic human fetuses.

A. DR computed on FRR series obtained from animal models

Data from an established pregnant sheep model of labor were retrospectively analyzed. A recent comprehensive review on the pregnant sheep model and its translational significance for human physiology, in particular for studies of the autonomic nervous system, can be found in [23]. The animal cohort consisted of nine normoxic and five spontaneously chronically hypoxic near-term pregnant sheep fetuses which underwent intermittent umbilical cord occlusions mimicking uterine contractions during labor. The animal and experimental models were described elsewhere [20]. Briefly, sheep fetuses were studied over a 6 hours period during which a mechanical stimulation was applied to the umbilical cord by using an inflatable silicon rubber cuff. After a baseline period (approximately 1 hour) with no stimulations, umbilical cord occlusions (UCOs) were delivered every 2.5 minutes and lasted for 1 minute. Three levels of occlusion strength, from partial to complete, were performed: mild (MILD, 60 minutes), moderate (MODERATE, 60 minutes) and complete (SEVERE, 2 hours or until pH < 7.00 was reached). The stimulation protocol ended with a recovery period. During the stimulation protocol, fetal arterial blood samples were collected with intervals of 20 minutes to quantify the values of pH, lactate and base deficit (hereafter referred to as "biomarkers").

Sheep fetuses were categorized as chronically hypoxic if $\mathrm{O_2Sat} < 55\%$, as measured before the beginning of the UCO stimulation protocol. In this study, we refer to the two models as "normoxic" and "chronically hypoxic", respectively. As per experimental protocol, both models showed a progressive worsening acidemia of the hypoxic status until pH < 7.00 was reached (Fig. 2).

0018-9294 (c) 2019 IEEE. Personal use is permitted, but republication/redistribution requires IEEE permission. See http://www.ieee.org/publications_standards/publications/rights/index.html for more information.

This article has been accepted for publication in a future issue of this journal, but has not been fully edited. Content may change prior to final publication. Citation information: DOI 10.1109/TBME.2019.2932808, IEEE Transactions on Biomedical Engineering

Fetal ECGs were collected by means of electrodes implanted into the left supra-scapular muscles, in the muscles of the right shoulder and in the cartilage of the sternum, and digitized at 1000 Hz. FRR series were automatically extracted from the fetal ECG [24].

1) FRR series preprocessing: A preprocessing similar to the one proposed in [19] was adopted for both datasets. Briefly, FRR series were analyzed to determine whether they were suitable for further analysis in terms of noise, by excluding those recordings with more than 10% gaps during MODERATE and SEVERE phases. Two healthy fetuses were excluded from the analysis because of the high amount of missing beats. Furthermore, FRR intervals greater than 1500 ms (40 bpm) were labeled as artifacts and substituted with an equivalent number of beats (calculated dividing the length of each artifact by the median of the 20 nearby FRR samples). These reconstructed samples were not used as anchor points in the PRSA analysis; however, they contributed to the selection of nearby anchor points.

2) Analyses performed: AC and DC were computed for several pairs of T and s values (with a constant value of $L = 50$), which were suggested as relevant in previous works. In particular, we considered:

- AC and DC with $T = 1$ and $s = 2$ [1];
- AC and DC with $T = 5$ and $s = 5$ [19];
- AC and DC with $T = 9$ and $s = 9$ [3];
- AC and DC with $T = 40$ and $s = 1$ [8] (acceleration and deceleration phase-rectified slopes, as recently introduced by Fanelli *et al.*, measure the slope of the PRSA at the anchor point position; we approximated their values using $s = 1$ in (2)).

DR was estimated using the aforementioned parameters values, but we also varied the value of s to verify its impact. In practice, DR was computed for: $T = 1$ with $s = 2$, $T = 5$ with $s = 1$ and $s = 5$, $T = 9$ with $s = 1$ and $s = 9$, and $T = 40$ with $s = 1$.

Two statistical analyses were performed on the values obtained. First, we computed the Spearman's correlation coefficients between AC, DC, DR and biomarkers, during the entire experiment, for each model separately. Second, we determined the discriminatory power of AC, DC and DR values in differentiating normoxic and chronically hypoxic sheep, by computing the area-under-ROC curve (AUC). We used a jackknife resampling scheme: in practice, each sheep was kept out iteratively and the AUC was computed on the remaining 11 ones. The values we reported are the mean and standard deviation of the 12 AUC values obtained.

Given the fact that in both animal models the standard deviation of the FRR signals increased during the protocol phases (Fig. 3a), and that such variation was correlated with the biomarkers (Fig. 3b), the changes in the power of the signal would have directly affected the values of AC and DC (PRSA is proportional to the standard deviation of the signal, see sec. II-A). Therefore, in order to detect changes in FRR not simply due to power variations, AC, DC and DR values were corrected for the power of the signal. In practice, we derived a linear model for each AC, DC and DR with standard deviation as the explanatory variable. The linear regression (with zero intercept) was obtained with the Theil-Sen method, which was shown to be robust to outliers and when there is heteroscedasticity [25], that in our case might arise due to the changes between phases in the experimental protocol (Fig. 3a). Once the model was estimated, the residuals between the data and model were used to determine the correlation and AUC aforementioned. In this way, the linear dependency between the power of the signal and AC, DC and DR was removed.

3) Results: AC, DC and DR varied across protocol phase in both animal models, as shown in Table I. A marked difference of DR during SEVERE with respect to BASELINE was evident, within the same animal model and across models. Of note, the normoxic and chronically hypoxic sheep fetuses had opposite average growing trends (DR for the normoxic fetuses was higher, than that of the chronically hypoxic ones).

Despite such marked changes across protocol phases, only few AC and DC values had a statistically significant correlation with the biomarkers (Table II), while most DR values had. In addition, correlations were highly variable.

Fig. 4 reports average and standard deviation of the AUC values for each of the fourteen parameters. DR displayed either comparable or higher discriminative power with respect AC and DC in each protocol phase. In particular, DR resulted with the highest AUC during SEVERE ($T = 5$ and $s = 1$ ranked first). Interestingly, AC, DC and DR with $T = 40$ and $s = 1$ were perfectly differentiating chronically hypoxic from normoxic fetuses during BASELINE.

B. CTU-UHB Intrapartum Cardiotocography Database

The CTU-UHB Intrapartum Cardiotocography Database from Physionet [21], [26] was used to test the DR index on human FHR data. It contains carefully selected cardiotocography recordings (CTG) of 552 fetuses (singleton, uncomplicated pregnancies, with no congenital defects and week of gestation ≥ 37) resampled at 4 Hz (for further details, please refer to [21]). Umbilical artery pH was also available for each fetus at birth. Forty-four fetuses had an umbilical artery pH value ≤ 7.05 and, in this study, were considered as acidotic.

1) CTG data preprocessing: Missing-beats were reconstructed using linear interpolation. A surrogated FRR series (in ms) was then derived by inverting and rescaling FHR CTG values. For each recording, we also estimated the FRR baseline using the Mantel *et al.*'s algorithm [27] and determined the decelerations according to [28].

For further analysis, only FRR series collected during 1 hour before the onset of delivery stage II, with less than 30% of missing beats, were considered. Overall, FRR data fulfilling these criteria were available for 24 acidotic and 441 healthy fetuses.

2) Analyses performed: AC, DC and DR were computed, with the same parameter values described in sec. III-A2 on the FRR signal, for each of the 465 recordings. As for the sheep data, interpolated samples were not allowed to be anchor points.

In this dataset, we determined the discriminatory power of DR in detecting fetal acidemia, defined by pH≤ 7.05 at birth, only after correcting for the standard deviation of the signal

0018-9294 (c) 2019 IEEE. Personal use is permitted, but republication/redistribution requires IEEE permission. See http://www.ieee.org/publications_standards/publications/rights/index.html for more information.

This article has been accepted for publication in a future issue of this journal, but has not been fully edited. Content may change prior to final publication. Citation information: DOI 10.1109/TBME.2019.2932808, IEEE Transactions on Biomedical Engineering

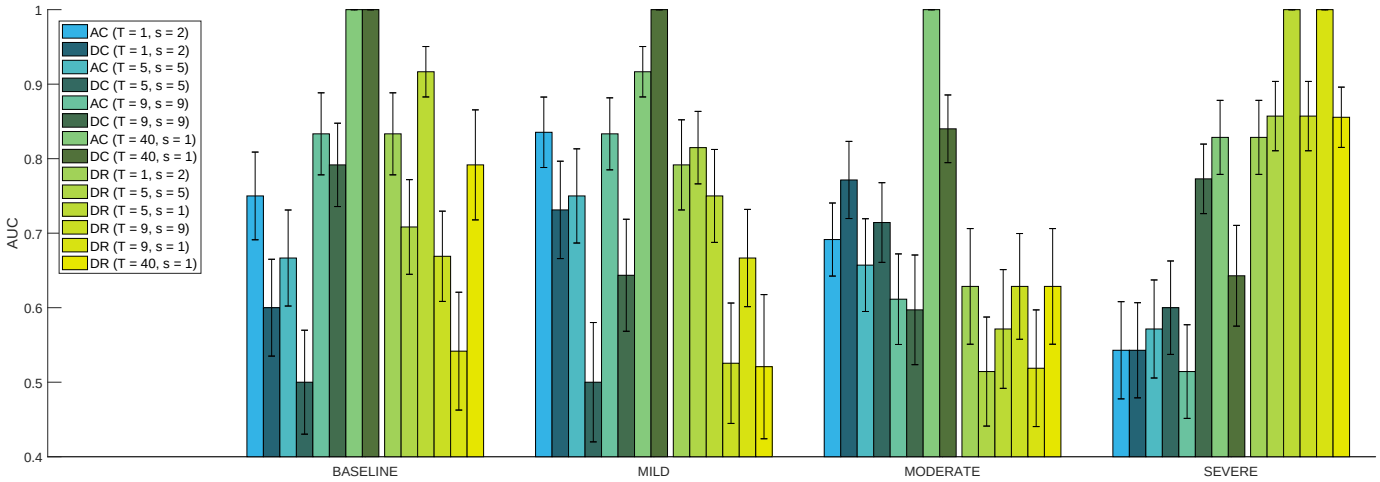

Fig. 4. Average and standard deviation of AUC values in discriminating normoxic and hypoxic sheep fetuses after power correction.

(given the proportional relation between the two quantities). However, during labor, FHR power is largely driven by decelerations, which differed in number, duration and amplitude in the data we considered (while in the animal model, given the strict experimental protocol, they were approximately homogeneous across the population). In particular, FHR decelerations were significantly different (Wilcoxon rank sum test; $p < 0.05$) between healthy and acidotic fetuses, when quantified in term of Deceleration Area (DA), a quantity recently found to be predictive of fetal acidemia [29]. Therefore, to remove the exogenous effect induced by differences in decelerations (and consequently power), instead of correcting for the standard deviation, we corrected for DA. The procedure we followed is the same described in sec. III-A2, in which the residuals of the linear regression between the variable and DA were further considered.

On this dataset, ROC analysis was performed for each index separately, similarly to what described in sec. III-A2. Then, features were ranked based on their average AUC.

3) Results: Similarly to what observed in the animal models (SEVERE in tab. I), the at-birth non-acidotic population had a higher DR for several T and s values (but statistical difference was observed only for $T = 1$ and $s = 2$, Wilcoxon rank sum test, $p < 0.05$). Fig. 5 depicts the average values of AUC for the fourteen DA-corrected indexes in descending order. Most of the values of DR ranked in the first positions, even if only DR with $T = 1$ and $s = 2$ displayed an AUC value higher than 0.6. DR with $T = 5$, which proved effective in the animal model, ranked second and third, respectively. Interestingly, most of AC and DC ranked in the last positions after their corresponding DR, highlighting DR (their difference) had a better discriminative power.

IV. Discussion

As we mathematically showed in section II-C, AC and DC were identical in absolute value for series generated by a stationary stochastic Gaussian process, and DR vanished. The situation was similar to what has been found on fetal RR series, when the heart rate of the fetus was measured in stationary conditions (for example during monitoring in clinical environment, far from labor) [3], [5]. Then, AC and DC values were found to be almost identical and, therefore, performed similarly in terms of risk stratification of the fetus.

When non-stationary signals were present, for example during labor, the PRSA series was affected by the low-frequency components of the UCOs. Consequently, DR was expected to differ from zero. The results we obtained on the animal models suggested that this was indeed true. During BASELINE, the values of AC and DC were similar in most of the cases for the normoxic model (Table I) while, during SEVERE, they significantly differed. Moreover, the correlation between DR and biomarkers was statistically significant for a larger set of parameters values, with respect to AC and DC, even after correcting for the power of the signal.

On the CTU-UHB data, DR proved to be the most discriminant parameter of acidosis at birth, and thus hypoxia during labor, and was superior to the AC and DC considered. In addition, DR with $T = 1$ and $s = 2$, $T = 5$ and s either 1 or 5, ranked first in the animal model too, and may deserve further investigations. However, it is possible that the small number of acidemic fetuses at birth in the CTU-UHB dataset might have limited our inference.

To the best of our knowledge, all previous works on AC and DC did not correct for the signal's power. However, our findings in (8), and their exemplification in section II-C, remarks that there is a direct linear dependence of the values of AC and DC with the standard deviation of the signal. The power of the signal thus acts as a confounding factor and without any correction, it was not possible to understand whether the differences found were due to true alterations of AC, DC and DR or simply to dissimilarities in the standard deviation. For this reason we corrected the values of AC, DC and DR with respect to the standard deviation of the FRR series, in the animal model data, and with respect to deceleration area in CTG data. DA is directly linked with the standard deviation of the FRR series, but it is a stronger predictor of acidemia at birth [29]. In our data, at-birth acidotic fetuses had a larger median DA (at-birth non-acidotic: 100.2

0018-9294 (c) 2019 IEEE. Personal use is permitted, but republication/redistribution requires IEEE permission. See http://www.ieee.org/publications_standards/publications/rights/index.html for more information.

This article has been accepted for publication in a future issue of this journal, but has not been fully edited. Content may change prior to final publication. Citation information: DOI 10.1109/TBME.2019.2932808, IEEE Transactions on Biomedical Engineering

beats vs at-birth acidotic: 193.5 beats, $p = 0.005$). Correcting for the standard deviation of the signal would have been equivalent, but we preferred DA as the number of decelerations is different in each signal (and not constant as in the animal model experimental protocol). Both with sheep and human fetuses data, we believe that we selected the methodological configuration that was less likely to produce false positive differences in AC, DC or DR between the different populations considered.

V. Limitations

The study bears some limitations which need to be acknowledged. First, in the animal model, the limited sample size could have influenced our results. We partly mitigated the issue by using a jackknife resampling scheme. Second, the RR series used in the animal model were derived from ECGs, while the CTG dataset was composed of FHR series. Previous studies [24] evidenced how RR series are more effective for the early detection of worsening acidemia, so the use of RR series also for human data should have been preferred (but were not available). Third, the values of T and s we considered were originally proposed either for the analysis of RR series (like [1], [19] and [3]), or for FHR series resampled at a fixed rate [8]. It was not the goal of the paper to select the best combination of T and s, so we did not investigated the effects of the different sampling rates on the parameter values. Fourth, in our analysis of the CTG data, we only considered the last hour of labor stage I to reduce the effects of signal loss and feto-maternal heart rate confusion [30] (common during stage II) on the estimates. A larger dataset would have been necessary for the selection of a significant number of recordings of sufficient quality, as done by Georgieva *et al.* [31], that studied the use of PRSA on the last 30 minutes of stage II labor. Finally, DR should be tested in other populations, also using multivariate models, which proved to be superior with respect to univariate-based classifiers [14], [15]. We plan to do so in the future.

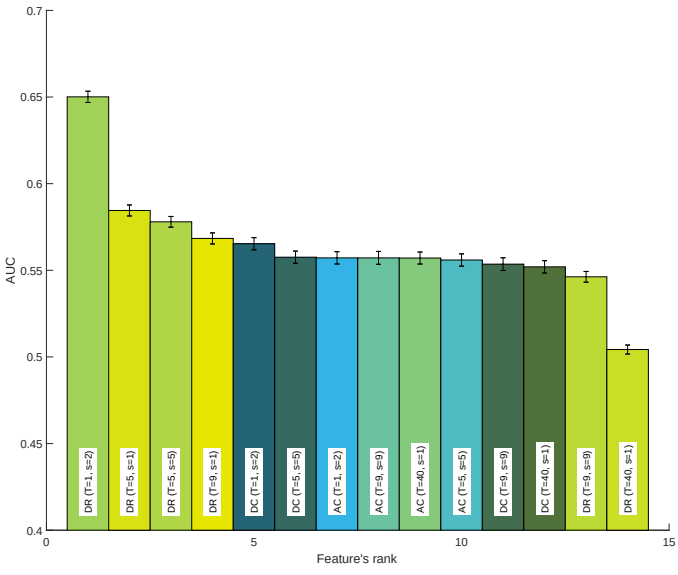

Fig. 5. AUC values (average and standard deviation) in discriminating fetuses, who at birth displayed a pH value ≤ 7.05, in the CTU-UHB Dataset.

VI. Conclusions

In this work, we presented a theoretical investigation of the PRSA series' properties by deriving a closed-form formula valid for series generated by stationary stochastic Gaussian process. The main finding was that the values of AC and DC are identical for these signals (in absolute value). The result motivated the introduction of a new index, *i.e.*, Deceleration Reserve, which emphasizes asymmetric growing and decaying HR trends and non-stationarity, such as those arising during uterine contractions. For this reason the metric is, by design, very interesting in the context of FHR analysis.

DR was tested first on two animal models of labor. During severe occlusions of the umbilical cord, DR was different between normoxic and chronically hypoxic fetuses and achieved high discriminatory power. In particular, after correcting for the power of the signal, DR was lower for the chronically hypoxic fetuses.

On CTG data coming from the CTU-UHB dataset, DR displayed a moderate discriminatory power between non-acidemic and acidemic fetuses at birth, suggesting that the autonomic regulation might be different under prolonged stress. Of note, DR performed better than AC and DC in this context, after correcting for the power of the signal.

To conclude, the study may open interesting scenarios for interpreting PRSA-based results and improving FHR monitoring and its related outcomes.

Appendix A
Number of Anchor Points

For a stationary stochastic Gaussian process, on average, half of the samples of any series are anchor points for DC, while the other half are anchor points for AC. In fact, using the terminology of section II-B, the stochastic scalar variable $\mathbf{g}^\intercal\mathbf{x}$ is normally distributed with zero mean and covariance matrix $\mathbf{g}^\intercal\mathbf{\Sigma_x}\mathbf{g}$, implying that the probability of a point to be an anchor for DC is

$$P(\mathbf{g}^\intercal\mathbf{x} > 0) = \frac{1}{2}\left(1 - \mathrm{erf}\left(-\frac{0}{\sqrt{2}\mathbf{g}^\intercal\mathbf{\Sigma_x}\mathbf{g}}\right)\right) = \frac{1}{2}.$$

Appendix B
Effect of Time Reversal

Given two stationary zero-mean stationary stochastic Gaussian processes X and Y, where Y is the time-reversed version of X, the acceleration-dictated PRSA series of Y is the time-reversed version of the deceleration-dictated PRSA series of X. Thus, -AC for Y is identical to DC for X. In fact, using the terminology of section II-B, the covariance matrix of Y is $\mathbf{\Sigma_y} = \mathbf{B}\mathbf{\Sigma_x}\mathbf{B}^\intercal$, where $\mathbf{B}$ is an anti-diagonal identity matrix.

0018-9294 (c) 2019 IEEE. Personal use is permitted, but republication/redistribution requires IEEE permission. See http://www.ieee.org/publications_standards/publications/rights/index.html for more information.

This article has been accepted for publication in a future issue of this journal, but has not been fully edited. Content may change prior to final publication. Citation information: DOI 10.1109/TBME.2019.2932808, IEEE Transactions on Biomedical Engineering

Then, considering that $\mathbf{B}$ is an orthogonal matrix, the PRSA series of Y is

$$\begin{aligned}\mathrm{PRSA}_{\mathbf{g}}^{Y}[i] &= \frac{2}{(2\pi)^L}\int\limits_{\mathbf{g}^\intercal\mathbf{y}>0}(\mathbf{e}_i^\intercal\mathbf{y})e^{-\frac{1}{2}\mathbf{y}^\intercal\boldsymbol{\Sigma}_{\mathbf{y}}^{-1}\mathbf{y}}d\mathbf{y}\\ &= \frac{2}{(2\pi)^L}\int\limits_{\mathbf{g}^\intercal\mathbf{B}\mathbf{x}>0}(\mathbf{e}_i^\intercal\mathbf{B}\mathbf{x})e^{-\frac{1}{2}\mathbf{x}^\intercal\boldsymbol{\Sigma}_{\mathbf{x}}^{-1}\mathbf{x}}d\mathbf{x}\\ &= \frac{2}{(2\pi)^L}\int\limits_{(-\mathbf{g}^\intercal)\mathbf{x}>0}(\mathbf{e}_{2L-i+1}^\intercal\mathbf{x})e^{-\frac{1}{2}\mathbf{x}^\intercal\boldsymbol{\Sigma}_{\mathbf{x}}^{-1}\mathbf{x}}d\mathbf{x}\\ &= \mathrm{PRSA}_{-\mathbf{g}}^{X}[2L-i+1].\end{aligned}$$

REFERENCES

[1] A. Bauer, J. W. Kantelhardt, P. Barthel, R. Schneider, T. Mkikallio, K. Ulm, K. Hnatkova, A. Schmig, H. Huikuri, A. Bunde, M. Malik, and G. Schmidt, "Deceleration capacity of heart rate as a predictor of mortality after myocardial infarction: cohort study," *Lancet*, vol. 367, pp. 1674–1681, 2006.

[2] A. Bauer, J. W. Kantelhardt, A. Bunde, P. Barthel, R. Schneider, M. Malik, and G. Schmidt, "Phase-rectified signal averaging detects quasi-periodicities in non-stationary data," *Physica A*, vol. 364, pp. 423–434, 2006.

[3] T. Stampalija, D. Casati, M. Montico, R. Sassi, M. W. Rivolta, V. Maggi, A. Bauer, and E. Ferrazzi, "Parameters influence on acceleration and deceleration capacity based on trans-abdominal ECG in early fetal growth restriction at different gestational age epochs," *Eur J Obstet Gynecol Reprod Biol*, vol. 188, pp. 104–112, 2015.

[4] C. Zou, H. Dong, F. Wang, M. Gao, X. Huang, J. Jin, B. Zhou, and X. Yang, "Heart acceleration and deceleration capacities associated with dilated cardiomyopathy," *Eur J Clin Invest*, vol. 46, pp. 312–320, 2016.

[5] S. M. Lobmaier, N. Mensing van Charante, E. Ferrazzi, D. A. Giussani, C. J. Shaw, A. Mller, J. U. Ortiz, E. Ostermayer, B. Haller, F. Prefumo, T. Frusca, K. Hecher, B. Arabin, B. Thilaganathan, A. T. Papageorghiou, A. Bhide, P. Martinelli, J. J. Duvekot, J. van Eyck, G. H. Visser, G. Schmidt, W. Ganzevoort, C. C. Lees, K. T. Schneider, C. M. Bilardo, C. Brezinka, A. Diemert, J. B. Derks, D. Schlembach, T. Todros, A. Valcamonico, N. Marlow, and A. van Wassenaer-Leemhuis, "Phase-rectified signal averaging method to predict perinatal outcome in infants with very preterm fetal growth restriction- a secondary analysis of TRUFFLE-trial," *Am J Obstet Gynecol*, vol. 215, pp. 630.e1–630.e7, 2016.

[6] T. Stampalija, D. Casati, L. Monasta, R. Sassi, M. W. Rivolta, M. L. Muggiasca, A. Bauer, and E. Ferrazzi, "Brain sparing effect in growth-restricted fetuses is associated with decreased cardiac acceleration and deceleration capacities: a case-control study," *BJOG*, vol. 123, pp. 1947–1954, 2016.

[7] W. Hu, X. Jin, P. Zhang, Q. Yu, G. Yin, Y. Lu, H. Xiao, Y. Chen, and D. Zhang, "Deceleration and acceleration capacities of heart rate associated with heart failure with high discriminating performance," *Sci Rep*, vol. 23, p. 23617, 2016.

[8] A. Fanelli, G. Magenes, M. Campanile, and M. G. Signorini, "Quantitative Assessment of Fetal Well-Being Through CTG Recordings: A New Parameter Based on Phase-Rectified Signal Average," *IEEE J Biomed Health Inform*, vol. 17, pp. 959–966, 2013.

[9] R. Sassi, T. Stampalija, D. Casati, E. Ferrazzi, A. Bauer, and M. W. Rivolta, "A methodological assessment of phase-rectified signal averaging through simulated beat-to-beat interval time series," *Comput Cardiol*, vol. 41, pp. 601–604, 2014.

[10] Q. Pan, G. Zhou, R. Wang, G. Cai, J. Yan, L. Fang, and G. Ning, "Do the deceleration/acceleration capacities of heart rate reflect cardiac sympathetic or vagal activity? A model study," *Med Biol Eng Comput*, vol. 54, pp. 1921–1933, 2016.

[11] M. Ursino and E. Magosso, "Role of short-term cardiovascular regulation in heart period variability: a modeling study," *Am J Physiol Heart Circ Physiol*, vol. 284, no. 4, pp. H1479–H1493, 2003.

[12] C. Karmakar, Y. Kimura, M. Palaniswami, and A. Khandoker, "Analysis of fetal heart rate asymmetry before and after 35 weeks of gestation," *Biomed Signal Process Control*, vol. 21, pp. 43–48, 2015.

[13] Q. Pan, G. Zhou, R. Wang, Y. Yu, F. Li, L. Fang, J. Yan, and G. Ning, "The degree of heart rate asymmetry is crucial for the validity of the deceleration and acceleration capacity indices of heart rate: A model-based study," *Comput Biol Med*, vol. 76, pp. 39–49, 2016.

[14] H. Gonçalves, A. P. Rocha, D. Ayres-de Campos, and J. Bernardes, "Linear and nonlinear fetal heart rate analysis of normal and acidemic fetuses in the minutes preceding delivery," *Med Biol Eng Comput*, vol. 44, pp. 847–855, 2006.

[15] P. Warrick, E. Hamilton, D. Precup, and R. Kearney, "Classification of Normal and Hypoxic Fetuses From Systems Modeling of Intrapartum Cardiotocography," *IEEE Trans Biomed Eng*, vol. 57, pp. 771–779, 2010.

[16] A. Petrozziello, I. Jordanov, A. T. Papageorghiou, W. G. Christopher Redman, and A. Georgieva, "Deep learning for continuous electronic fetal monitoring in labor," in *Conf Proc IEEE Eng Med Biol Soc*, 2018, pp. 5866–5869.

[17] Z. Cömert and A. F. Kocamaz, "Fetal hypoxia detection based on deep convolutional neural network with transfer learning approach," in *Software Engineering and Algorithms in Intelligent Systems*, R. Silhavy, Ed. Cham: Springer International Publishing, 2019, pp. 239–248.

[18] S. Tagliaferri, A. Fanelli, G. Esposito, F. G. Esposito, G. Magenes, M. G. Signorini, M. Campanile, and P. Martinelli, "Evaluation of the Acceleration and Deceleration Phase-Rectified Slope to Detect and Improve IUGR Clinical Management," *Comput Math Methods Med*, vol. 2015, pp. 1–9, 2015.

[19] M. W. Rivolta, T. Stampalija, D. Casati, B. S. Richardson, M. G. Ross, M. G. Frasch, A. Bauer, E. Ferrazzi, and R. Sassi, "Acceleration and Deceleration Capacity of Fetal Heart Rate in an In-Vivo Sheep Model," *PLoS ONE*, vol. 9, p. e104193, 2014.

[20] A. Xu, L. D. Durosier, M. G. Ross, R. Hammond, B. S. Richardson, and M. G. Frasch, "Adaptive Brain Shut-Down Counteracts Neuroinflammation in the Near-Term Ovine Fetus," *Front Neurol*, vol. 5, p. 110, 2014.

[21] V. Chudáček, J. Spilka, M. Burša, P. Janků, L. Hruban, M. Huptych, and L. Lhotská, "Open access intrapartum CTG database," *BMC Pregnancy Childbirth*, vol. 14, p. 16, 2014.

[22] J. W. Kantelhardt, A. Bauer, A. Y. Schumann, P. Barthel, R. Schneider, M. Malik, and G. Schmidt, "Phase-rectified signal averaging for the detection of quasi-periodicities and the prediction of cardiovascular risk," *Chaos Interdiscip J Nonlinear Sci*, vol. 17, pp. 015 112–015 112–9, 2007.

[23] J. L. Morrison, M. J. Berry, K. J. Botting, J. R. T. Darby, M. G. Frasch, K. Gatford, D. A. Giussani, C. L. Gray, R. Harding, E. A. Herrera, M. W. Kemp, M. C. Lock, I. C. McMillen, T. J. Moss, G. C. Musk, M. H. Oliver, T. R. H. Regnault, C. T. Roberts, J. Y. Soo, and R. L. Tellam, "Improving pregnancy outcomes in humans through studies in sheep," *Am J Physiol Regul Integr Comp Physiol*, vol. 315, no. 6, pp. R1123–R1153, 2018.

[24] L. D. Durosier, G. Green, I. Batkin, A. J. Seely, M. G. Ross, B. S. Richardson, and M. G. Frasch, "Sampling rate of heart rate variability impacts the ability to detect acidemia in ovine fetuses near-term," *Front Pediatr*, vol. 2, no. 38, 2014.

[25] R. Wilcox, "A note on the TheilSen regression estimator when the regressor is random and the error term is heteroscedastic," *Biom J*, vol. 40, no. 3, pp. 261–268, 1998.

[26] A. L. Goldberger, L. A. N. Amaral, L. Glass, J. M. Hausdorff, P. C. Ivanov, R. G. Mark, J. E. Mietus, G. B. Moody, C.-K. Peng, and H. E. Stanley, "PhysioBank, PhysioToolkit, and PhysioNet: Components of a New Research Resource for Complex Physiologic Signals," *Circulation*, vol. 101, pp. e215–e220, 2000.

[27] R. Mantel, H. P. van Geijn, F. J. Caron, J. M. Swartjes, E. E. van Woerden, and H. W. Jongsma, "Computer analysis of antepartum fetal heart rate: 1. baseline determination," *Int J Biomed Comput*, vol. 25, no. 4, pp. 261–272, 1990.

[28] J. Pardey, M. Moulden, and C. W. Redman, "A computer system for the numerical analysis of nonstress tests," *Am J Obstet Gynecol*, vol. 186, no. 5, pp. 1095–103, 2002.

[29] A. G. Cahill, M. G. Tuuli, M. J. Stout, J. D. López, and G. A. Macones, "A prospective cohort study of fetal heart rate monitoring: deceleration area is predictive of fetal acidemia," *Am J Obstet Gynecol*, vol. 218, no. 5, pp. e1–523.e12, 2018.

[30] T. Stampalija, M. Signaroldi, C. Mastroianni, E. Rosti, V. Signorelli, D. Casati, and E. M. Ferrazzi, "Fetal and maternal heart rate confusion during intra-partum monitoring: comparison of trans-abdominal fetal electrocardiogram and doppler telemetry," *J Matern Fetal Neonatal Med*, vol. 25, no. 8, pp. 1517–1520, 2012.

[31] A. Georgieva, A. T. Papageorghiou, S. J. Payne, M. Moulden, and C. W. G. Redman, "Phase-rectified signal averaging for intrapartum electronic fetal heart rate monitoring is related to acidaemia at birth," *BJOG*, vol. 121, no. 7, pp. 889–894, 2014.

0018-9294 (c) 2019 IEEE. Personal use is permitted, but republication/redistribution requires IEEE permission. See http://www.ieee.org/publications_standards/publications/rights/index.html for more information.